Journal of the Optical Society of America B

OPTICAL PHYSICS

Dual-pump frequency comb generation in normally dispersive optical fibers

AKU ANTIKAINEN* AND GOVIND P. AGRAWAL

The Institute of Optics, University of Rochester, Rochester, New York 14627, USA
**Corresponding author: aku.antikainen@rochester.edu*

Received 26 May 2015; revised 30 June 2015; accepted 1 July 2015; posted 1 July 2015 (Doc. ID 241534); published 22 July 2015

We show that tunable frequency combs can be generated by launching two continuous-wave pumps at slightly different wavelengths into a normally dispersive optical fiber. The dual-pump configuration allows the tuning of comb spacing into the terahertz regime. Different pump powers and frequency separations are explored numerically to determine the effect of the input parameters on frequency comb generation. The relative power of the two pumps is found to be a critical factor through its crucial effect on optical wave breaking. The pump powers and fiber length are shown to have a significant effect on the comb width as well. Unlike in the case of supercontinuum generation, Raman scattering is found to have a negligible or even a slightly detrimental effect. Our findings also help bridge the gap between work done on the propagation of a single pulse and the evolution of dual-pump signals in normally dispersive highly nonlinear fibers.

OCIS codes: (320.7140) Ultrafast processes in fibers; (190.4370) Nonlinear optics, fibers.

http://dx.doi.org/10.1364/JOSAB.32.001705

1. INTRODUCTION

Frequency combs offer a direct link between optical and microwave frequencies [1] and have applications in diverse technological areas such as precision metrology [2,3], optical communications [4], and pulse-train generation [5]. The spectrum of a mode-locked laser is an obvious example of what could be considered a frequency comb, but such a spectrum lacks both tunability and wavelength span. Modulating a continuous wave (CW) electronically offers a convenient way to generate a tunable frequency comb, but the small spectral width of the resulting comb is a clear drawback. Moreover, the upper limit of comb spacing is limited to 40–50 GHz by the speed of the electronics used.

Nonlinear optics is often employed to generate wider frequency combs. In 1984, Hasegawa suggested using induced modulation instability (MI) to generate a train of short optical pulses with tunable repetition rates and durations [6]. Chernikov *et al.* advocated the use of two CW pumps at slightly different wavelengths in the anomalous-dispersion regime of optical fibers and generated a train of solitons with a 114 GHz repetition rate [7]. High-repetition-rate pulse trains have also been generated through rational harmonic mode locking [8] and pulse train multiplication [9]. Modulation instability inside a ring cavity was employed by Nakazawa *et al.* with pulsed pumping [10]. In 2001, Coen and Haeltermann used a CW pump for the same observation [11]. Ring cavities are promising for producing pulse trains with rates exceeding 500 GHz [12]. More recently, numerous studies have demonstrated the potential of microring resonators for producing frequency combs [13,14]. Although these results are impressive and the methods to achieve them undeniably clever, some applications outside of optical communications require even higher comb spacings in the THz regime [15–17].

Photonic crystal fibers (PCFs) have been used in recent years for supercontinuum generation by pumping them in the anomalous-dispersion regime [18,19]. This technique does not produce high-quality frequency combs because ultrashort solitons undergo Raman-induced frequency shifts [20] that are highly dependent on the duration of the solitons. The resulting optical spectrum inherently blurs into a supercontinuum in an uncontrollable manner because of Raman-induced cross talk that is phase sensitive for ultrashort solitons [21]. The lack of coherence in supercontinua generated through MI can be attributed to the fact that the MI is seeded by noise in the case of a narrow initial spectrum. This incoherence can be partially overcome through a dual-pump input signal. This approach avoids spontaneous MI and generates sidebands that are separated by the initial frequency difference of the two input CW signals. Indeed, Fatome *et al.* demonstrated the generation of pulse trains with repetition rates ranging from 1.5 THz to an impressive 3.4 THz [22].

Even though anomalous dispersion is known to lead to a wider supercontinuum, significant spectral broadening from self-phase modulation (SPM) can be observed in the normal dispersion regime of an optical fiber as well. Indeed, supecontinua have been produced using normally dispersive fibers [23,24]. The dual-pump configuration, with one pump in the anomalous and the other in the normal dispersion regime, has also been studied [25]. A detailed analytical and numerical comparison of dual-pump dynamics in the normal and anomalous dispersion regimes using a simplified model has been provided by Trillo *et al.* [26]. A more recent theoretical and experimental study by Fatome *et al.* focused on the time-domain effects of optical wave breaking in the dual-pumping configuration with weak normal dispersion [27]. The study used a model that neglects the third- and higher-order dispersive terms, the Raman effects, and the frequency-dependence of the nonlinearity but provided excellent agreement between experiments and numerical simulations, as care was taken to ensure the validity of the model in the experimental setup.

Since most applications do not require the frequency comb to be a train of solitons in the time domain, anomalous dispersion has no clear advantage over normal dispersion, aside from a possibly broader comb. On the other hand, the normal dispersion regime offers increased robustness that is due to the absence of Raman-shifted solitons and MI-amplified noise. Furthermore, the normal dispersion regime has been shown to have a beneficial impact on spectral flatness in the context of supercontinuum generation [28]. The aim of this study is to demonstrate that dual CW pumps can be used in the normal dispersion regime of a PCF to generate tunable frequency combs. We explore the parameter space through extensive numerical simulations and determine the effect of different input parameters on the comb width. Optical wave breaking is shown to play a key role in producing spectral broadening of the frequency comb. Raman effects, often ignored in most studies of frequency combs, are included. We discuss the conditions under which their neglect is justified.

2. NUMERICAL MODEL

To study the generation of frequency combs inside an optical fiber, we use the generalized nonlinear Schrödinger equation that has been used extensively for studying supercontinuum generation and shown to be accurate down to the few-cycle regime [18]. It can be written in the form [19]

$$\frac{\partial A}{\partial z}+\frac{\alpha}{2}A-\sum_{n\geq 2}\frac{i^{n+1}}{n!}\beta_n\frac{\partial^n A}{\partial T^n} = i\gamma\left(1+i\tau_s\frac{\partial}{\partial T}\right)\left(A(z,T)\int_{-\infty}^{\infty}R(T')|A(z,T-T')|^2\mathrm{d}T'\right), \tag{1}$$

where A is the complex amplitude of the electric field, $T = t - z/v_g$ is the retarded time in a frame moving with the group velocity v_g, α accounts for fiber losses, and γ is the nonlinear parameter. Further, the sum is over dispersive terms of second and higher orders whose impact is governed by the parameters β_n defined as $\beta_n = (d^n\beta/d\omega^n)$ and evaluated at the central frequency of the incident optical signal.

The right side of Eq. (1) governs all the nonlinear effects. The nonlinear response function, $R(t) = 0.82\delta(t) + 0.18h_R(t)$, includes both the delayed Raman response h_R and the instantaneous Kerr-type electronic response [19]. The Raman contribution is modeled through the full experimental Raman spectrum of silica [29]. Self-steepening is governed by the shock time scale τ_s.

In our numerical simulations, two CW input beams are launched simultaneously into a PCF exhibiting normal dispersion at both of the pump frequencies. Figure 1 shows the dispersion curve for our fiber with its zero-dispersion wavelength at 1133 nm. Both pump wavelengths are chosen to be shorter than this to ensure normal dispersion. Since the PCF lengths in our studies are ~10 m, we ignore fiber losses for simplicity by setting $\alpha = 0$. We used $\gamma = 15$ W/km and $\tau_s = 0.563$ fs in our simulations. The dispersion parameters are found from the curve given in Fig. 1.

The dual-pump input comes from two CW lasers, one at the frequency $\nu_0 = c/\lambda_0$ with $\lambda_0 = 1060$ nm and another at a higher frequency $\nu_0 + \nu_m$. The two pump wavelengths were chosen near 1060 nm because of the availability of powerful lasers as well as normally dispersive highly nonlinear fibers in this wavelength range. The dual-pump input field can be written as

$$A(0,T) = \frac{\sqrt{P_0}}{\sqrt{1+x}}\left[1+\sqrt{x}\,\exp(-2i\pi\nu_m T)\right] + a_n(0,T), \tag{2}$$

where P_0 is the total pump power, x is the ratio of the power at the higher frequency CW pump to that of the lower frequency CW pump, and $a_n(0,T)$ is the input quantum noise that was incorporated in the form of one noise photon per mode [30]. In our simulations x is varied from 0 to 1, P_0 from 1 to 300 W, and ν_m from 25 GHz to 1 THz. Different shot noise seeds were tried for each sets of parameters, but the effect of the input noise was found to be negligible on the resulting spectra. It should be noted that, although our simulations have been done for the CW initial conditions, the results are applicable to pulses longer than 100 ps since the numerical time window was 40 ps wide. Experimental verification of our results will

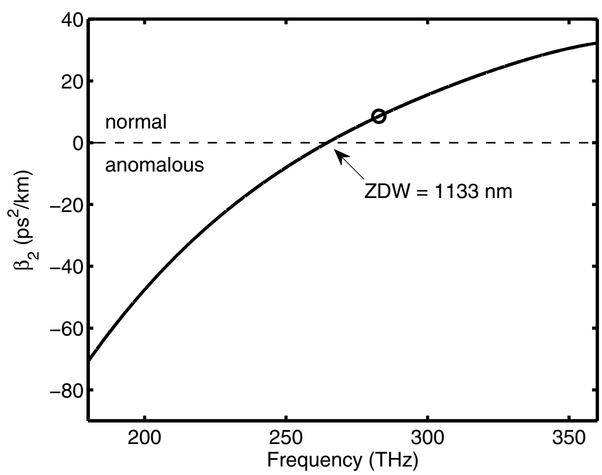

Fig. 1. Dispersion parameter β_2 as a function of optical frequency. The circle denotes the lower frequency pump at 1060 nm. The zero-dispersion wavelength (ZDW) of the PCF is 1133 nm.

require such pulsed lasers to realize peak power levels near 100 W.

3. ROLE OF OPTICAL WAVE BREAKING

We begin by considering the values $P_0 = 200$ W and $x = 1$, corresponding to two pumps with equal powers of 100 W, and assume that the pumps are separated by $\nu_m = 350$ GHz. Figure 2 shows the evolution of such a dual-pump signal over a PCF length of 5 m by showing the optical spectra and temporal profile at certain locations in the fiber chosen to highlight the importance of optical wave breaking (OWB) in the comb-formation process. Initially at $z = 0$, the spectrum consists of two spectral lines. In the time domain, we see a sinusoidal pattern resulting from beating of the two CW pumps. From Eq. (2), these sinusoidal power variations have the form

$$P(0, T) = |A(0, T)|^2 \approx P_0\left[1 + \frac{2\sqrt{x}}{1+x}\cos(2\pi\nu_m T)\right], \quad (3)$$

where the small shot noise terms have been left out. The modulation depth $d_m = 2\sqrt{x}/(1+x)$ has its maximum value of 1 for $x = 1$, the case shown in Fig. 2. We will see later that reduced values of d_m for $x \neq 1$ affect the comb evolution significantly.

The crucial role of OWB in separating two regimes of evolution in the context of single-pulse supercontinuum generation in normally dispersive fiber was pointed out by Finot *et al.* [28]. More recently, Fatome *et al.* showed that a double shock is formed in the dual-pumping configuration at the initial modulation minima and that optical undular bores can be observed after such a double shock [27]. Similar double-shock formation can be seen in Fig. 2. At a distance of 3.5 m, a frequency comb has been formed, but its −50 dB width is limited to about 10 THz. The temporal trace shows that the double shock has not yet occurred at 3.5 m but has taken place at a distance of 4 m, as evidenced by the sharp dips at the location of intensity minima. At a distance of 4.25 m, intense temporal peaks are formed at the shock positions because of the simultaneous presence of multiple frequency components. These components mix nonlinearly to produce new frequency components, and this four-wave mixing then manifests itself as the spectral side lobes that emerge after the double shock formation. As the spectrum before the shock formation is a comb, the emerging side lobes consist of discrete frequencies that contribute to the width of the comb. This can clearly be seen in Fig. 2 at a distance of 5 m, where the frequency comb has a −50 dB bandwidth of about 25 THz. Since the whole comb stays in the normal-dispersion regime of the fiber over its entire length, neither soliton dynamics nor modulation instability contributes to the comb formation or spectral broadening.

As the double-shock formation takes place at the initial modulation minima of the dual-pump signal, the initial modulation depth d_m could be expected to have an effect on the shock formation and on the resulting frequency comb. Figure 3 shows the evolution under conditions identical to that of Fig. 2 except for unequal pump powers such that $x = 0.1$ and $d_m = 0.575$. A direct comparison of the two figures shows the drastic impact on the comb generation when the modulation depth is decreased even if the modulation remains very significant. A comb is still produced through SPM, but its −50 dB width is smaller by a factor of about 2. At a distance of 3.75 m, modulation depth is somewhat reduced in the time domain. For longer distances, OWB takes place, and the edges of adjacent pulses collide with one another. However, the temporal intensity slope of the colliding edges is smaller, which leads to both suppressed spectral broadening and smaller temporal peak powers for the forming intensity peaks. The resulting frequency comb at a distance of 5 m is significantly narrower compared to the case of equal-power pumps shown in Fig. 2. Clearly, deeper initial modulation helps create broader frequency combs.

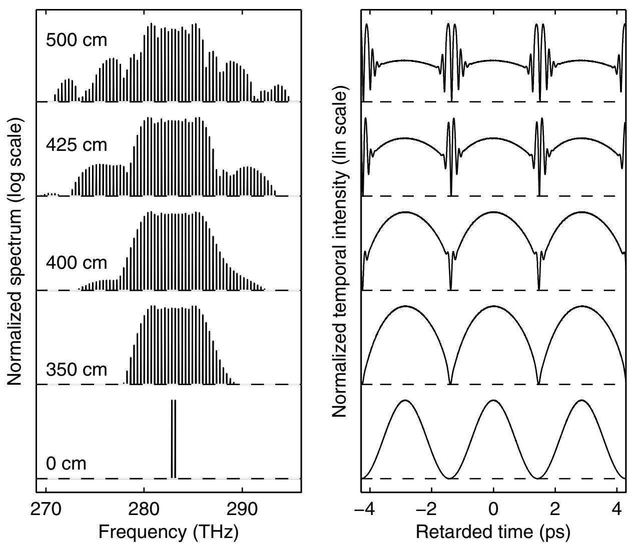

Fig. 2. Spectral (left) and temporal (right) evolution of a dual-pump signal in the normal dispersion regime over 5 m of PCF. The spectrum scale is logarithmic over a 50-dB range. The dashed horizontal lines show the −50 dB level for the spectra and the zero level for the temporal intensity plotted on a linear scale. Parameter values for the two CW pumps are $P_0 = 200$ W, $x = 1$, and $\nu_m = 350$ GHz.

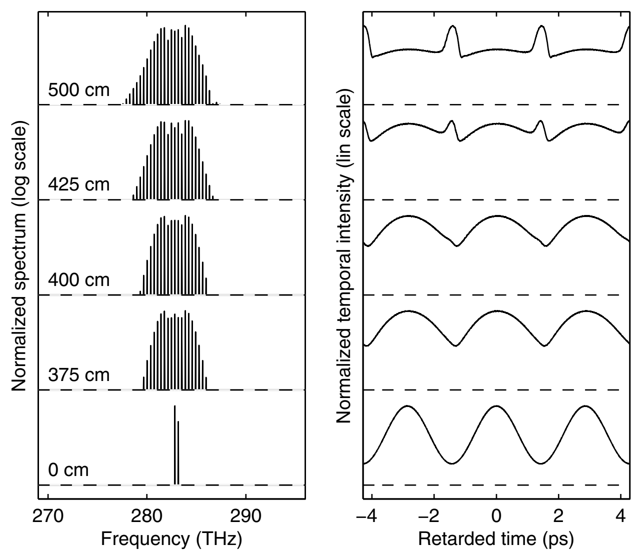

Fig. 3. Same as Fig. 2 but for unequal pump powers such that $x = 0.1$. The total pump power is the same in both cases.

Figures 2 and 3 both show more and more spectral broadening with increasing propagation distance. One may ask whether ultrawide frequency combs can be produced by simply increasing the PCF length. The answer is negative for several reasons. First, too long of a propagation distance will be detrimental because of the amplification of noise through four-wave mixing. Second, Raman scattering may begin to impact the quality of frequency combs. Third, fiber losses, although neglected here, could limit the performance for long fibers. To study how the comb width depends on various input parameters, we have carried out a large number of numerical simulations. We used them to calculate the comb width defined as the bandwidth containing 99.98% of the total spectral power such that only 0.01% of the total power lies on each side of this frequency band. We also checked that the spectra can indeed be considered frequency combs and were not ordinary supercontinua by verifying that at least 99.99% of the total spectral power was concentrated at the discrete comb frequencies. This rather uncommon definition of the spectral width was chosen over the more traditional measures (such as FWHM or −10 dB bandwidth) because the latter work well only for spectra of similar shapes. The spectra observed in this study can be structurally different for different input parameters (see the output spectra in Figs. 2 and 3). Furthermore, a simple dB threshold width measure is unable to account for spectral broadening happening below the threshold, and this broadening can be very significant. For example, in Fig. 2 the −10 dB spectral width barely changes upon propagation from 350 to 500 cm, while the spectrum does in fact still evolve and broaden quite drastically upon propagation.

Keeping in mind our definition of the comb bandwidth, Fig. 4 shows the numerically calculated comb bandwidth as a function of propagation distance and pump-power ratio x using $P_0 = 200$ W and $\nu_m = 700$ GHz. For a given value of x, spectral broadening starts immediately and is fairly linear up to a certain distance, after which intense broadening occurs over a short distance. The initial linear broadening is consistent with SPM-induced spectral broadening [19], and the abrupt sudden broadening can be explained in terms of OWB. The features seen in the figure also bear considerable resemblance to the observations on spectral broadening of a single pulsed pump in [28], in which abrupt spectral broadening was also explained in terms of OWB. In our case, the ratio of the pump powers plays a role analogous to that of the peak power of the pulse.

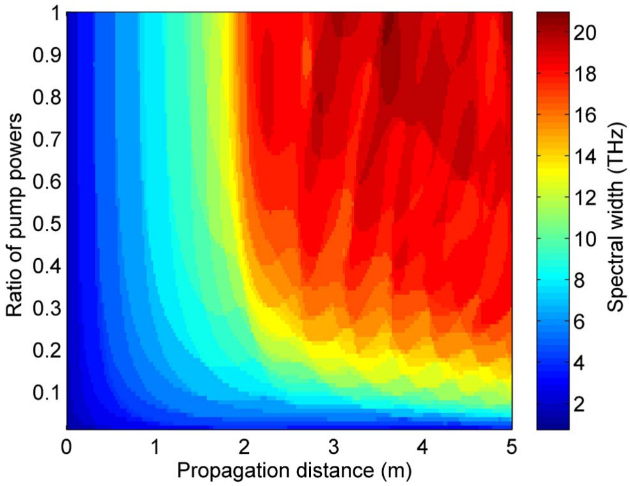

Fig. 4. Comb bandwidth (color encoded) as a function of the ratio of pump powers and propagation distance. The input parameters are $P_0 = 200$ W and $\nu_m = 700$ GHz.

4. PUMP POWER AND PROPAGATION DISTANCE

The total pump power is known to have a significant effect on supercontinuum generation, where it sets the order of soliton for pulses propagating in the anomalous dispersion regime of an optical fiber. We thus expect the total pump power P_0 to influence frequency comb generation in the normal dispersion regime of our PCF. In the case of a single pulse, it is customary to characterize the relative importance of dispersion and nonlinearity through the use of the dispersion length $L_D = T_0^2/|\beta_2|$ and the nonlinear length $L_{\mathrm{NL}} = 1/(\gamma P_0)$, where T_0 is a measure of pulse duration and P_0 is the pulse's peak power. In our dual-pumping configuration, total pump power P_0 and the period of sinusoidal modulations $T_0 = 1/\nu_m$ play the role of the corresponding two parameters. For the input parameters used in Figs. 2–4, the nonlinear length is always smaller than the dispersion length, usually by orders of magnitude. Thus, the nonlinear effects dominate over the dispersive effects, similar to the case of supercontinuum generation. Furthermore, for a dual-pump input signal one might expect dispersion to be less of an issue than for a single pulse, as every frequency component of the electric field is present in every time slot that has a duration of the input period, and the average power over a period stays almost constant throughout propagation. One might then expect that nonlinear power transfer between different frequencies can continue occurring throughout the evolution of a dual-pump signal. Thus, instead of exploring the evolution dynamics as a function of propagation distance in meters, it is more intuitive to normalize the distance as $\xi = z/L_{\mathrm{NL}}$ using the nonlinear length.

Figure 5 shows the comb bandwidth as a function of ξ and pump power P_0. The comb width increases quite monotonically with respect to both of these parameters. What is noteworthy is that, although a certain power level is required to achieve a specific comb width, low initial powers cannot be compensated for by making the fiber longer. Furthermore, for low pump powers and longer propagation distances, Raman scattering is able to transfer a significant portion of the initial power at the pump frequencies to a continuum at lower frequencies. Since low input powers create narrow combs, higher-order dispersion plays no role in the comb formation, and other than the Raman-induced power transfer, the evolution of a low-power dual-pump signal is very similar to that observed in [26].

5. EFFECT OF RAMAN SCATTERING

Not all nonlinear power-transfer mechanisms contribute to the formation of a frequency comb. Spontaneous Raman scattering is responsible for transferring power from the pump frequencies to a broader band of lower frequencies [19]. Such a transfer of power is obviously detrimental in the context

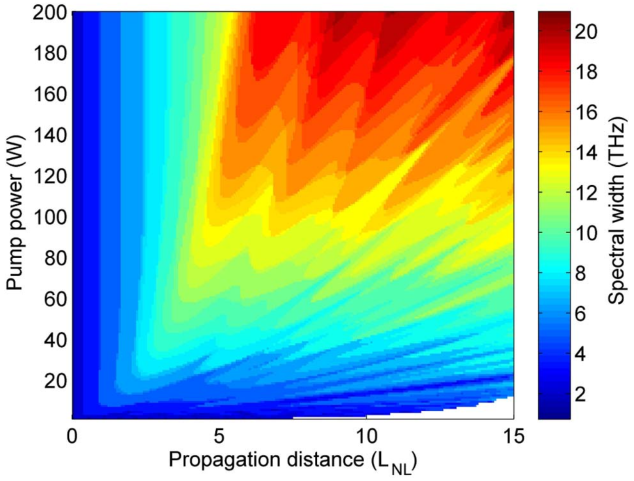

Fig. 5. Comb bandwidth (color encoded) as a function of total pump power and propagation distance. The input parameters are $x = 1$ and $\nu_m = 700$ GHz. Spectra that did not qualify as frequency combs have been left out (lower right corner).

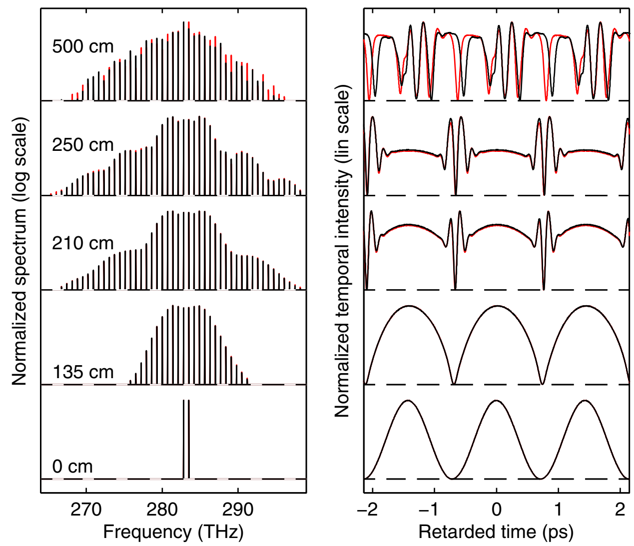

Fig. 7. Same as Fig. 6 but with $P_0 = 200$ W, $x = 1$, and $\nu_m = 700$ GHz.

of frequency comb generation. The emergence of a continuum decreases the contrast between the comb and the background. Furthermore, because power is being transferred away from the pump frequencies, the strength of beneficial nonlinear effects decreases as well. Thus, Raman scattering could be detrimental even when the comb spectrum is narrow enough such that the peak of the Raman gain lies outside of the comb bandwidth.

To study the effect of Raman scattering on the comb formation, we performed simulations with the Raman contribution turned off by setting $R(T') = \delta(T')$ in Eq. (1). Figure 6 shows the evolution of a 5 W dual-pump signal over 100 m both with (black) and without (red) the Raman effect. It is obvious that the effect of Raman scattering is negligible for this specific set of pump parameters. In numerical simulations, a Raman peak was observed when the Raman effect was included, but its spectral power was below −70 dB at 13.2 THz below the lower pump frequency. Similar behavior was observed for many other pump powers and frequency separations. Only when the total pump power exceeded 200 W, Raman scattering played a slightly more significant role. As an example, Fig. 7 shows evolution over 5 m of PCF using the parameter values $P_0 = 200$ W, $x = 1$, and $\nu_m = 700$ GHz.

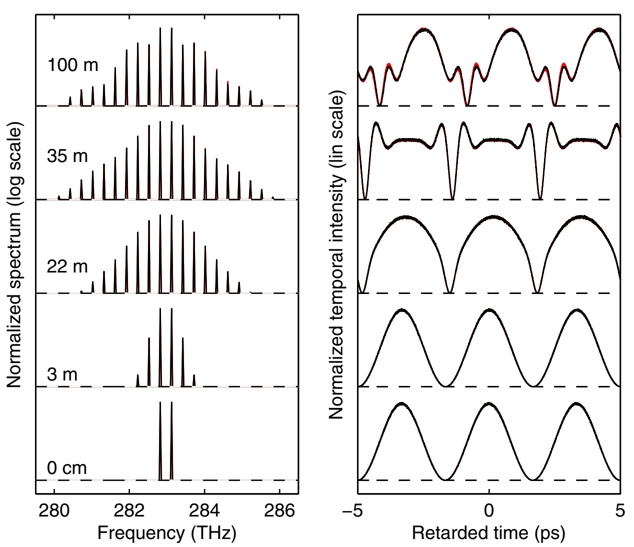

Fig. 6. Evolution of a dual-pump signal over 100 m with (black lines) and without (red lines) including the Raman effect. Pump parameters are $P_0 = 5$ W, $x = 1$, and $\nu_m = 300$ GHz. The scale for spectra is logarithmic, ranging from −60 to 0 dB. The effect of Raman scattering is negligible in this case.

In this case, the maximum comb width is reached at a propagation distance of 2.5 m, and before that the effect of Raman scattering on the spectral and temporal evolution is almost completely negligible. For larger propagation distances, the spectra and the temporal intensity profiles start to differ more. In particular, the comb spectrum becomes asymmetric with slightly more power at red-shifted frequencies. This is expected since high-frequency components pump the low-frequency components through stimulated Raman scattering.

The comb spectrum after 5 m of propagation also appears slightly broader when Raman scattering is included. However, it should be kept in mind that the spectra are normalized. The apparent broadening is due to a Raman-induced power transfer from the pump frequencies and nearby sidebands to a continuum of frequencies. Even though the Raman-amplified band stays well below the −70 dB level compared to the pump frequencies, this power transfer is enough to lower the central frequency peaks with respect to the peaks at the comb edge, thus making the normalized spectrum appear wider. By examining the unnormalized spectra, we found that the spectrum was actually broader when Raman scattering was not included. We thus conclude that in the dual-pumping configuration in the normal dispersion regime of a fiber the effect of Raman scattering is either negligible or slightly detrimental. This is a noteworthy difference between comb generation and supercontinuum generation. In the context of supercontinuum generation in normally dispersive fiber, Raman scattering is an important physical phenomenon that helps extend the continuum toward lower frequencies. In comb generation, however, Raman scattering does not contribute to the comb width even when the Raman gain band overlaps with the comb.

6. CONCLUSIONS

We have shown through numerical simulations that tunable frequency combs can be generated by launching two CW pumps at slightly different wavelengths into a normally dispersive optical fiber. The numerical model is based on the generalized nonlinear Schrödinger equation that has been used extensively for studying supercontinuum generation. The dual-pump configuration produces a periodic sinusoidal modulation and allows tuning of the comb spacing from tens of gigahertz into the terahertz regime. Our results show that the relative powers of the two pumps play a critical role, and the widest frequency combs form when the two pumps are launched with the same power. The reason behind this is related to the phenomenon of optical wave breaking known to occur in the case of normal dispersion.

In order to quantify the usefulness of the proposed scheme, we studied the dependence of the comb bandwidth on several important input parameters such as the total power, relative powers, frequency separation of the two pumps, and the length of the fiber employed. The depth of sinusoidal modulation produced by beating of the two pumps was shown to have a crucial effect on comb width, with deeper modulation enabling broader combs. This was interpreted and explained through the crucial role of optical wave breaking in SPM-induced spectral broadening. Unlike the case of supercontinuum generation, Raman scattering was found to have a negligible or even a slightly detrimental effect on comb generation. This is in sharp contrast to the case of supercontinuum generation where Raman scattering plays an essential role.

Experimental verification of our results would require two lasers whose wavelengths lie in the normal dispersion of the fiber and are spaced apart by a few nanometers. The use of CW lasers with power levels exceeding 100 W may prove impractical. However, such power levels are easily attainable if Q-switched lasers emitting nanosecond pulses are employed. Our results apply to this situation. The use of semiconductor lasers should allow the adjustment of the wavelength separation through temperature tuning, resulting in the formation of tunable frequency combs.

Funding. Fulbright Center Finland; Suomalainen Tiedeakatemia (Finnish Academy of Science and Letters).

REFERENCES

1. S. A. Diddams, D. J. Jones, J. Ye, S. T. Cundiff, J. L. Hall, J. K. Ranka, R. S. Windeler, R. Holzwarth, Th. Udem, and T. W. Hänsch, "Direct link between microwave and optical frequencies with a 300 THz femtosecond laser comb," Phys. Rev. Lett. **84**, 5102–5105 (2000).
2. Th. Udem, R. Holzwarth, and T. W. Hänsch, "Optical frequency metrology," Nature **416**, 233–237 (2002).
3. B. Bernhardt, A. Ozawa, P. Jacquet, M. Jacquey, Y. Kobayashi, Th. Udem, R. Holzwarth, G. Guelachvili, T. W. Hänsch, and N. Picqué, "Cavity-enhanced dual-comb spectroscopy," Nat. Photonics **4**, 55–57 (2009).
4. J. Pfeifle, V. Brasch, M. Lauermann, Y. Yu, D. Wegner, T. Herr, K. Hartinger, P. Schindler, J. Li, D. Hillerkuss, R. Schmogrow, C. Weimann, R. Holzwarth, W. Freude, J. Leuthold, T. J. Kippenberg, and C. Koos, "Coherent terabit communications with microresonator Kerr frequency combs," Nat. Photonics **8**, 375–380 (2014).
5. C.-B. Huang, Z. Jiang, D. E. Leaird, and A. M. Weiner, "High-rate femtosecond pulse generation via line-by-line processing of phase-modulated CW laser frequency comb," Electron. Lett. **42**, 1114–1115 (2006).
6. A. Hasegawa, "Generation of a train of soliton pulses by induced modulational instability in optical fibers," Opt. Lett. **9**, 288–290 (1984).
7. S. V. Chernikov, E. M. Dianov, D. J. Richardson, R. I. Laming, and D. N. Payne, "114 Gbit/s soliton train generation through Raman self-scattering of a dual frequency beat-signal in dispersion decreasing optical fibre," Appl. Phys. Lett **63**, 293–295 (1993).
8. N. Onodera, A. J. Lowery, L. Zhai, Z. Ahmed, and R. S. Tucker, "Frequency multiplication in actively modelocked semiconductor lasers," Appl. Phys. Lett. **62**, 1329–1331 (1993).
9. I. Shake, H. Takara, S. Kawanishi, and M. Saruwatari, "High-repetition-rate optical pulse generation by using chirped optical pulses," Electron. Lett. **34**, 792–793 (1998).
10. M. Nakazawa, K. Suzuki, and H. Haus, "Modulation instability oscillation in nonlinear dispersive ring cavity," Phys. Rev. A **38**, 5193–5196 (1988).
11. S. Coen and M. Haeltermann, "Continuous-wave ultrahigh-repetition-rate pulse-train generation through modulational instability in a passive fiber cavity," Opt. Lett. **26**, 39–41 (2001).
12. A. Zadok, J. Sendowski, and A. Yariv, "Birefringence-induced trains of high-rate pulses in a mode-locked fiber laser," IEEE Photon J. **1**, 128–134 (2009).
13. Y. Okawachi, K. Saha, J. S. Levy, Y. Henry Wen, M. Lipson, and A. L. Gaeta, "Octave-spanning frequency comb generation in a silicon nitride chip," Opt. Lett. **36**, 3398–3400 (2011).
14. A. R. Johnson, Y. Okawachi, J. S. Levy, J. Cardenas, K. Saha, M. Lipson, and A. L. Gaeta, "Chip-based frequency combs with sub-100 GHz repetition rates," Opt. Lett. **37**, 875–877 (2012).
15. A. M. Weiner, D. E. Leaird, G. P. Wiederrecht, and K. A. Nelson, "Femtosecond pulse sequences used for optical manipulation of molecular motion," Science **247**, 1317–1319 (1990).
16. D. Umstadter, E. Esarey, and J. Kim, "Nonlinear plasma waves resonantly driven by optimized laser pulse trains," Phys. Rev. Lett. **72**, 1224–1227 (1994).
17. Y. Liu, S.-G. Park, and A. M. Weiner, "Enhancement of narrow-band terahertz radiation from photoconducting antennas by optical pulse shaping," Opt. Lett. **21**, 1762–1764 (1996).
18. J. M. Dudley, G. Genty, and S. Coen, "Supercontinuum generation in photonic crystal fiber," Rev. Mod. Phys. **78**, 1135–1184 (2006).
19. G. P. Agrawal, *Nonlinear Fiber Optics*, 5th ed. (Academic, 2013).
20. F. M. Mitschke and L. F. Mollenauer, "Discovery of the soliton self-frequency shift," Opt. Lett. **11**, 659–661 (1986).
21. A. Antikainen, M. Erkintalo, J. M. Dudley, and G. Genty, "On the phase-dependent manifestation of optical rogue waves," Nonlinearity **25**, R73–R83 (2012).
22. J. Fatome, S. Pitois, C. Fortier, B. Kibler, C. Finot, G. Millot, C. Courde, M. Lintz, and E. Samain, "Multiple four-wave mixing in optical fibers: 1.5–3.4-THz femtosecond pulse sources and real-time monitoring of a 20-GHz picosecond source," Opt. Commun. **283**, 2425–2429 (2010).
23. H. Sotobayashi and K. Kitayama, "325 nm bandwidth supercontinuum generation at 10 Gbit/s using dispersion-flattened and non-decreasing normal dispersion fibre with pulse compression technique," Electron. Lett. **34**, 1336–1337 (1998).
24. A. Hartung, A. M. Heidt, and H. Bartelt, "Design of all-normal dispersion microstructured optical fibers for pulse-preserving supercontinuum generation," Opt. Express **19**, 7742–7749 (2011).
25. P.-A. Champert, V. Couderc, P. Leproux, S. Février, V. Tombelaine, L. Labonté, P. Roy, C. Froehly, and P. Nérin, "White-light supercontinuum generation in normally dispersive optical fiber using original multi-wavelength pumping system," Opt. Express **12**, 4366–4371 (2004).

26. S. Trillo, S. Wabnitz, and T. A. B. Kennedy, “Nonlinear dynamics of dual-frequency-pumped multiwave mixing in optical fibers,” Phys. Rev. A **50**, 1732–1747 (1994).
27. J. Fatome, C. Finot, G. Millot, A. Armaroli, and S. Trillo, “Observation of optical undular bores in multiple four-wave mixing,” Phys. Rev. X **4**, 021022 (2014).
28. C. Finot, B. Kibler, L. Provost, and S. Wabnitz, “Beneficial impact of wave-breaking for coherent continuum formation in normally dispersive nonlinear fibers,” J. Opt. Soc. Am. B **25**, 1938–1948 (2008).
29. R. H. Stolen, J. P. Gordon, W. J. Tomlinson, and H. A. Haus, “Raman response function of silica-core fibers,” J. Opt. Soc. Am. B **6**, 1159–1166 (1989).
30. P. D. Drummond and J. F. Corney, “Quantum noise in optical fibers. I. Stochastic equations,” J. Opt. Soc. Am. B **18**, 139–152 (2001).